Chaos, Solitons & Fractals 56 (2013) 145–153

Contents lists available at ScienceDirect

Chaos, Solitons & Fractals

Nonlinear Science, and Nonequilibrium and Complex Phenomena

journal homepage: www.elsevier.com/locate/chaos

Effects of neighborhood type and size in spatial public goods game on diluted lattice

Hong-yang Li [a,b], Jian Xiao [a], Yu-meng Li [a,b], Zhen Wang [a,c,*]

[a] Computational Social Science Lab, School of Innovation Experiment, Dalian University of Technology, Dalian 116024, China
[b] School of Information and Communication Engineering, Dalian University of Technology, Dalian 116024, China
[c] School of Software, Dalian University of Technology, Dalian 116621, China

ARTICLE INFO

Article history:

ABSTRACT

In this paper, we show in detail a picture of the effects of neighborhood type and size on cooperation promotion in the framework of spatial public goods game. First, we explore the role of learning and interaction neighborhood via the information flow rate and the cooperator-cluster stability. Extensive simulation results indicate that learning neighbors at the rising stage is to facilitate the information exchange and to promote cooperation among agents; at the gliding stage, learning neighborhood destroys cooperative clusters and accelerates the extinction of cooperators. Opposite to learning neighbors, interaction neighbors at the rising stage pull down the cooperation fraction; at the gliding stage, they help to maintain cooperative cluster and prohibit a further decrease in F_c. Then we review this issue on a microscopic level — snapshot pattern. We find several interesting results, through intermediate states, on the pattern formation towards the final state. Cooperators in a larger interaction size case will squeeze defectors and make their existence as a form of thin line; while the cooperative cluster in a larger learning neighborhood displays more 'blurry burs' at the boundaries, indicating an instability of cooperative clusters. Current results are of interest for us to further understand the cooperator persistence in many natural, social and economic systems.

1. Introduction

In recent years, how to interpret the widespread cooperation phenomenon among 'rational players' in many natural and socio–economical systems has become a popular issue in the scientific community [1,2]. The interactions between individuals can often appear by means of a game which represents a social dilemma. In general, social dilemmas often characterize the conflict between the individual and collective benefits in which any rational individual maximizes its benefit by choosing the defection, whereas the cooperation is optimal for the whole community [3,4]. Along the pioneering line of research, the incentive to investigate the collective cooperation has given rise to different mechanisms [5], including the consideration of age structure [6–8], complex interaction networks [9–13], the influence of noise [14–17], heterogeneous activity and ability [18–20], asymmetric payoff [21], payoff weighting [22–25], environment influence [26,27], aspiring to the fittest [28] and differences in evolutionary time scales [29]. In the classical framework, the evolutionary game theory is often employed to formulate and illustrate the emergence of cooperation. The prisoner's dilemma game (PDG), which was first conducted by Nowak and May [30], is a classical paradigm to probe the origin and evolution of cooperation. However, the public goods game (PGG) [31,33] is the best candidate to depict the interactions of a group of individuals and such kind of situation is quite common in reality, such as climate change, public traffic, stock market, etc. Two opposite strategies are identified: cooperation (C) if the player contributes to the

* Corresponding author at: Computational Social Science Lab, School of Innovation Experiment, Dalian University of Technology, Dalian 116024, China.
E-mail address: wangz@dlut.edu.cn (Z. Wang).

0960-0779/$ - see front matter © 2013 Elsevier Ltd. All rights reserved.
http://dx.doi.org/10.1016/j.chaos.2013.08.001

common pool or defection (D) if the player betrays others. Obviously, individuals are tempted to defect, while the group as a whole is best off if everybody cooperates. Failure to harvest the benefits of a collective investment and mindless exploitation of public goods are in fact the key causes for the 'tragedy of the commons'.

Aside from the progress in promoting altruism described above, graph theory provides a natural and very convenient framework to describe the population structure on which the evolution of cooperation is studied [32,34,35]. In the PGG model, the average benefit will decrease if the group size increases, which makes the cooperation benefits in larger groups more dependent on others' contributions and in a riskier consequence [36]. However, larger neighborhood size will ensure to get involved in more PGG rounds, which results in higher potential payoff. Recently, many scholars haven focused on the influence of network structure and unsymmetrical neighborhood [37]. On one hand, it has been found that the cooperation can be greatly promoted if the players are often placed on regular lattices or networks where the players can form some type of cooperative clusters to resist the exploitation of the defectors [38,39]. On the other hand, the fraction of cooperators is greatly enhanced due to disordered environments, i.e, vacant nodes in the community [40]. Wang et al. show that spatial reciprocity peaks in the vicinity of the percolation threshold, irrespective of network topological details [41] and strategy updating rules [42]. In the meanwhile, there have been different results under various game models with respect to neighborhood size and type. For the PDG model, Xia [43] finds the medium-sized neighborhood allows cooperators to thrive and substantially favors the evolution of cooperation; Ifti [39] discovers the critical average degree of nodes for which defection is the final state does not depend on network size, but only on the network topology; and that clustering is the mechanism which makes the development of cooperation possible; In Ref. [44], the cooperation is modified substantially in a way resembling a coherence-resonance-like behavior when the number of learning edges is increased; Players in ref [45] can have an adaptive neighbor size and individuals with low interaction intensity usually hold the boundary of cooperator cluster. For the snowdrift game model [46], Xiao et al. [47] investigates whether different neighborhood types are conducive to enhancing the cooperation for small disordered degree. Inspired by the previous works, we consider different neighborhood types (interaction or learning) and sizes in the community, and explore the role of neighborhood during different population densities. Through systematic simulations, we demonstrate that larger interaction and smaller learning neighbor size will enhance the stability of cooperator clusters. Moreover, we also study the effect of neighborhood on a microscopic level and unveil the process where cooperators exploit defectors through a cluster-forming mechanism.

The rest of this paper is organised as follows. In the next section, we give an introduction to the spatial public goods game model. In Section 3, the simulation results and discussions from three aspects are provided. Finally, concluding remarks are drawn in Section 4.

2. Model

We employ the spatial public goods game on a square lattice of size L^2 with the periodic boundary condition, where only a fraction of the nodes are occupied by players while the others are vacant. The random dilution of the lattice is performed only at the start of the game, and initially every individual x acts either as a cooperator or a defector with equal probability. At each round, every cooperator contributes the same cost to the common pool. Then the collected benefit is multiplied by a synergy factor, which denotes the enhancement effect created by cooperation. Then the resulting amount in the pool is shared by all players within the community. Hence, the net payoff for each cooperator P_C or defector P_D can be derived as follows:

$$P_C = \frac{rcN_c}{N} - c \tag{1}$$

$$P_D = \frac{rcN_c}{N} \tag{2}$$

where N_c is the number of cooperators in the community with total N players, c denotes the cost invested by each cooperator and r the synergy factor. Our Monte Carlo simulations are carried out comprising the following two steps.

First, an individual x obtains its payoff $P_x^g(t)$ at a certain Monte Carlo step (MCS) by playing the public goods game with player g, who is within player x's interaction realm. Therefore, the overall payoff of player x in a round should be added up from its first interaction neighbour to the last one, i.e, $P_x(t) = \sum_i P_x^i(t)$. Second, after computing all the payoffs of each player, player x randomly chooses player y within its learning realm and imitates the strategy of the chosen player according to the Fermi rule [9], i.e, the strategy transform probability at MCS t:

$$Pr\{s_x(t) \leftarrow s_y(t)\} = \frac{1}{1 + e^{\frac{P_x(t) - P_y(t)}{K}}} \tag{3}$$

where $s_x(t)$, $s_y(t)$ represent the strategy (C or D) of node x and y, $P_x(t)$, $P_y(t)$ denote their total payoff or fitness, and K indicates the amplitude of environment noise, such as errors and irrationality of individuals. If $K \gg 1$, player x will imitate the strategy of player y with almost 50% probability regardless of player y's fitness. When $K \to 0$, player x will mimic player y with very high probability given $P_x(t) < P_y(t)$, and there is little chance to imitate if $P_x(t) > P_y(t)$. To sum up, positive values of K indicate that better-behaved players are more likely to be imitated, but there always exists a small chance to accept a less successful strategy.

The distribution of one's neighbour range is described in Fig. 1. We define two different types of neighbours – *interaction neighbours* (*IN*) who affect the measurement of a player's overall payoff and *learning neighbours* (*LN*) who decide how many agents it can choose to adopt a new strategy. In this model, the neighbor size of *IN*,*LN* can be 4, 8, 12, 20. In case that a player has no neighbour within its reachable area, then it is 'frozen' and does not get

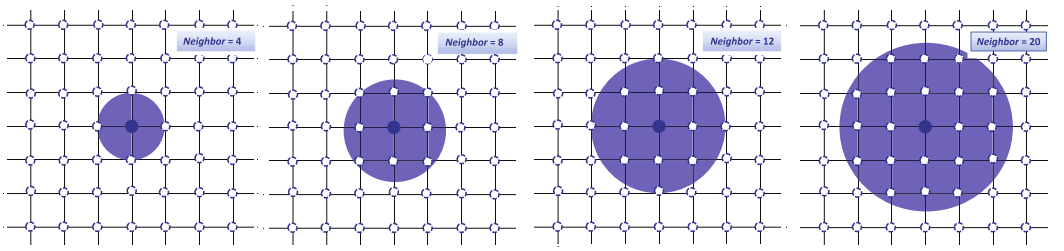

Fig. 1. The distribution of one's interaction or learning neighbor range.

involved in all steps. This scenario can appear when the population density and the range of neighbours are small, which means the scarce players are blocked out by empty nodes and can't receive or pass on strategy to others. The quantity N and N_c in Eqs. (1) and (2) are within the realm of interaction neighborhood. Since IN varies in different scenarios, for fair comparison, we adjust the value of synergy factor proportionally according to different INs, i.e, the ratio $\gamma = r/IN = \text{const}$.

To examine how the neighborhood size and type affect the cooperative evolution, we define the fraction of cooperators at step t as follows:

$$F_c(t) = \frac{\sum_x s_x(t)}{\rho L^2} \tag{4}$$

where $s_x(t)$ is 1 for cooperation and 0 for defection, ρ indicates the total population density during one simulation and L denotes the network size. Since our main interest resides in the final stationary state, i.e, $F_c = \lim_{t\to\infty} F_c(t)$, we use the *steady* cooperator fraction F_c as the main target in the following. In what follows, we set the network size L to be 200 or 600; the cost c each cooperator contributes in a round is constant to be 1; as the same in ref [35], the noise parameter K in Eq. (3) is fixed at 0.5; the ratio γ is fixed to be 0.7. To ensure accuracy, the cooperator fraction F_c is acquired by averaging over 10 samples, each of which is achieved by averaging the last 5,000 MCS among the total 80,000 steps.

3. Simulation results and discussions

3.1. Effect of learning neighborhood

By fixing the interaction size, we first explore the influence of learning neighborhood on cooperation evolution. Fig. 2 shows how the cooperator fraction varies as a function of population density, under different learning sizes while IN is fixed to be 4.

The variation of F_c over population density has three stages – the *rising*, the *smoothing* and the *falling* period. Each curve increases monotonously as population density becomes greater and achieves its maximum value of 1 when the population density reaches an arrival threshold ρ^*_{at}. When ρ is small, the information is not well spread and the cooperation strategy cannot be transmitted due to limited players. Then the curves enter into a smoothing process where the final state is in the domination of cooperators. As more agents appear, the network becomes active and clusters form bigger clusters to resist defectors. As ρ grows larger, the proportion of cooperators begins

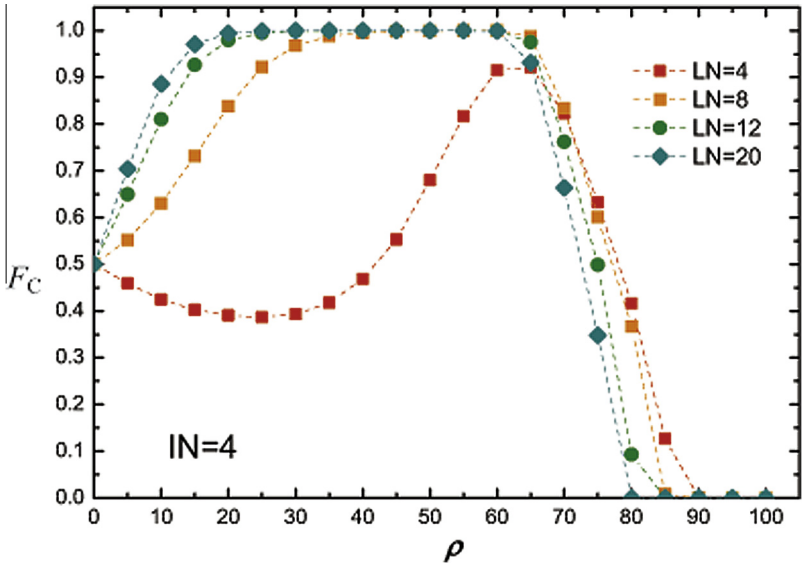

Fig. 2. The fraction of cooperators F_c as a function of population density ρ. Each curve stands for a different learning size. $IN = 4$; Network size $L = 600$.

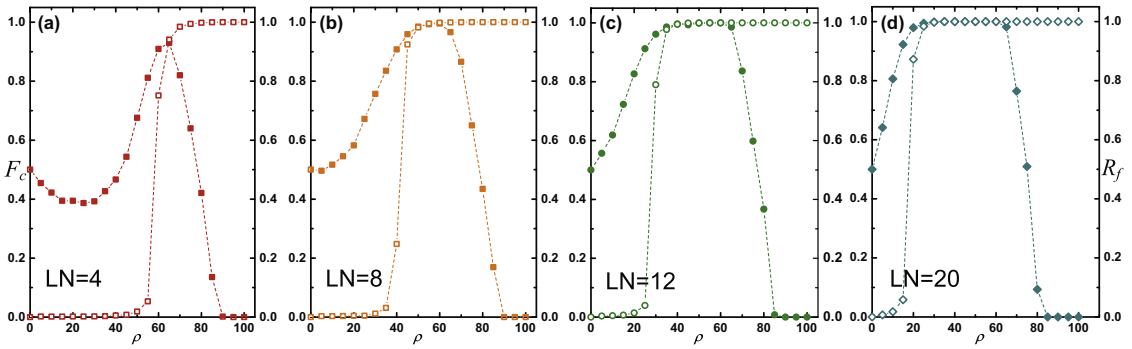

Fig. 3. The fraction of cooperators F_c and information flow rate R_f as a function of population density. Solid dots represent F_c, and hollow ones stand for R_f. The learning size in (a)–(d) is 4, 8, 12, 20, respectively; The interaction neighborhood size $IN = 4$; Network size $L = 200$.

to fall (a gliding threshold, ρ^*_{gt}) and the defectors predominate the community in the stationary state when ρ tends to be 1 (an extinction threshold, ρ^*_{et}). When the population density tends to 100%, defectors and cooperators are too close and cooperator clusters are easily broken by the benefit temptation of free riders. Note that the $LN = 4$ curve is different from others, which we will discuss later.

To investigate the intrinsic reason why the arrival threshold ρ^*_{at} differs under different LN sizes, we define the *information flow rate* in the stationary state as follows:

$$R_f = \frac{N_{cluster}}{\rho L^2} \tag{5}$$

where $N_{cluster}$ is the maximum number of players whose learning realms overlap with each other. The flow rate is the proportion of the number of players, in the maximum cluster, who can learn and imitate other players' strategy via learning links. Hence R_f serves as a metric as to how efficiently the information in the community can spread. Once the network initiation is settled, the value of the flow rate at each population point is fixed.

Fig. 3 shows the relationship of cooperator fraction and information flow rate in different learning sizes. From Fig. 3(b) to (d), the point at which F_c reaches its maximum value is in accordance with that where R_f also achieves its maximum. That is to say, the size of learning neighborhood decides at which population point the community's information fully flows among agents and cooperators can dominate in the final state. There is a slight difference in Fig. 3(a). The cooperator fraction reaches its maximum of 0.92 at population density 65%, whereas the flow rate reaches 1 at 75%. The influence of interactive neighbors cannot be ignored when learning size is relatively small compared with interaction size. To sum up, the information rate reaches its maximum at a smaller population when LN turns larger; the role of learning neighborhood at the incipient stage is to facilitate the exchange of information and the propagation of cooperation.

To further examine the role of learning neighborhood from another perspective, we define the *degree of stability* of cooperator cluster in the stationary state as follows:

$$D_s = 1 - \frac{\Delta N_{c\_final}}{N_{c\_final}} \tag{6}$$

where N_{c_final} represents the number of cooperators and ΔN_{c_final} denotes the number of the change from cooperators

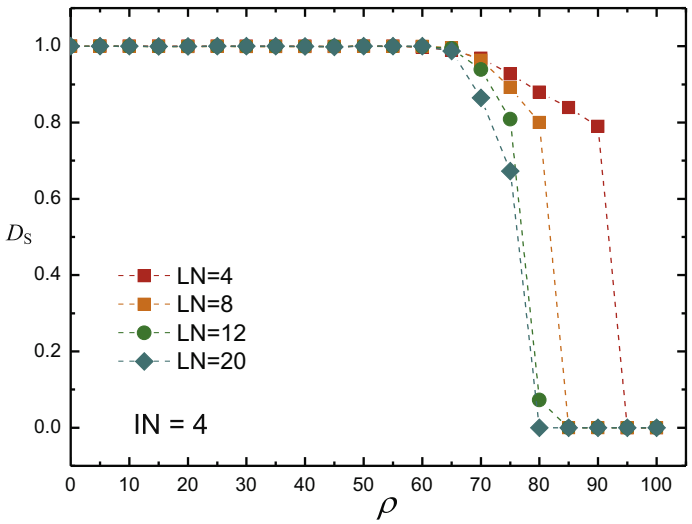

Fig. 4. The degree of stability D_s as a function of population density ρ. Each curve stands for a different learning size. Interaction size $IN = 4$; Network size $L = 200$.

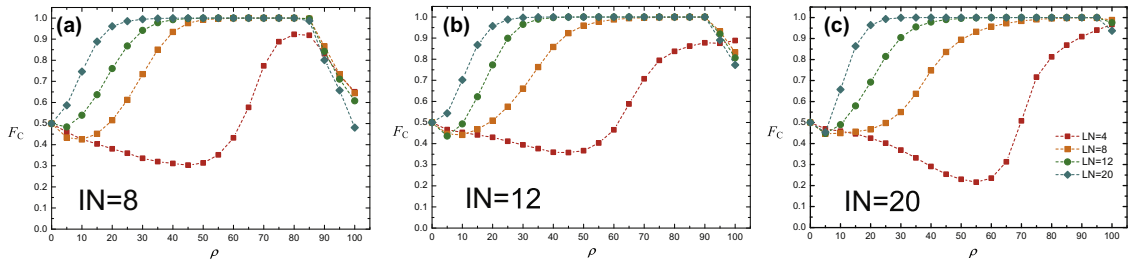

Fig. 5. The fraction of cooperators F_c as a function of population density ρ. The interaction size in (a)–(c) is 8, 12, 20, respectively; Network size $L = 600$.

to defectors in the final state. Note that the community is in a dynamical equilibrium, i.e, ΔN_{c_final} remains the same while the alteration of identities happens all the time. In case that F_c is 0 and all players are defectors, the cooperator-cluster stability is at the lowest level — we set D_s to be 0. Therefore, the degree of stability serves as a measurement to evaluate how stable the cooperator-cluster is.

Fig. 4 highlights the stability level over population density. At the initial stage, the cooperator cluster is stable, regardless of different learning sizes. As ρ grows lager beyond ρ^*_{gt}, the network becomes quite turbulent and D_s falls to 0 quickly, corresponding to the extension threshold. Therefore, larger learning size at the gliding stage enhances the network unstability and accelerates the extinction of cooperators at a smaller population density.

To verify the two theories above, we display the cooperator fraction under other *IN* sizes in Fig. 5.

It is obvious that at the rising stage larger learning size enhances the strategy flow among agents and helps the formation of the final cooperator-dominant state at a smaller ρ; while at the gliding period, smaller learning size maintains the network stability and impedes the exploitation of defectors. We can see a slight decrease is universal for all values of *IN* and *LN* when the population is below 10%. There exist many isolated individuals in the community when most nodes are empty, and the cooperation strategy is not effectively spread among them. Hence the few existing links between players enable defectors to exploit cooperators without having to fear the consequence of spatial reciprocity. In addition, due to the limited range

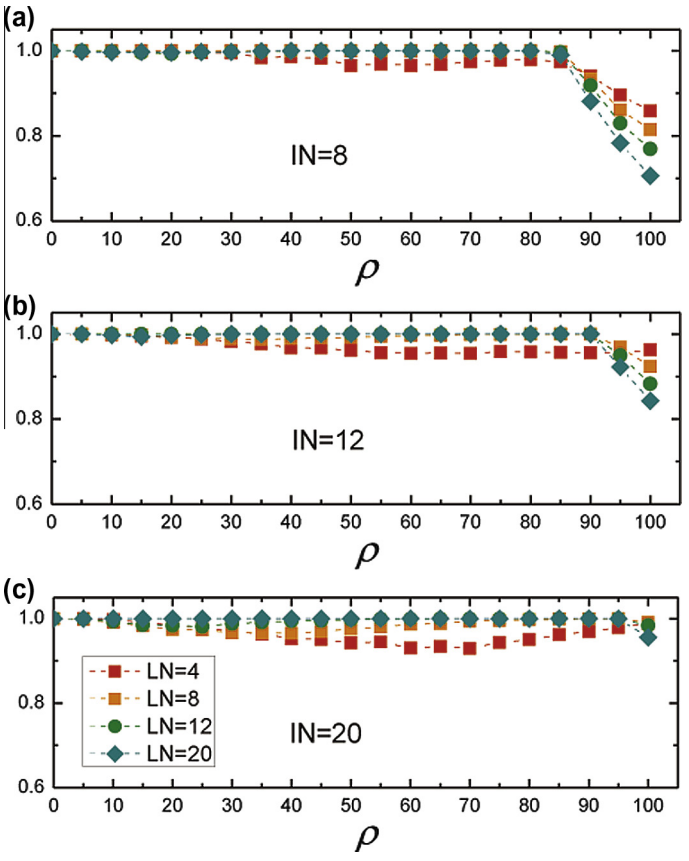

Fig. 6. The degree of stability D_s as a function of population density ρ. The interaction size in (a)–(c) is 8, 12, 20, respectively; Network size $L = 200$.

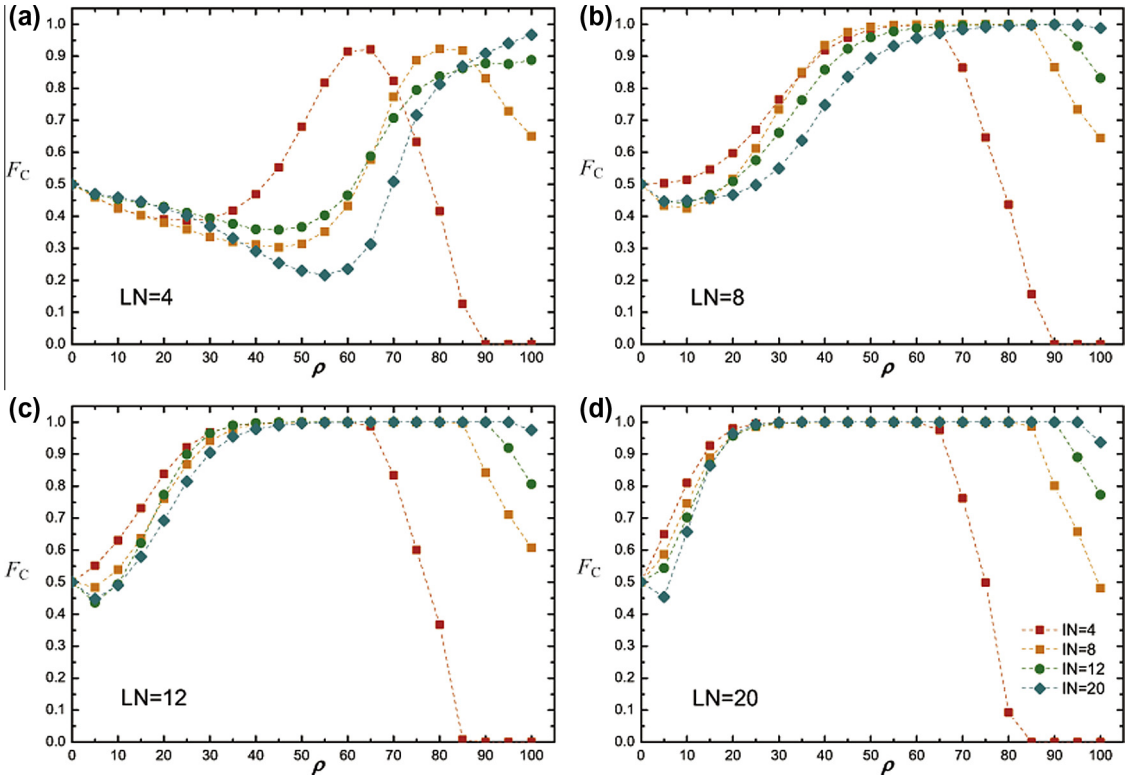

Fig. 7. The fraction of cooperators F_c as a function of population density ρ. Each curve stands for a different interaction size. The learning size in (a)–(d) is 4, 8, 12, 20, respectively; Network size $L = 600$.

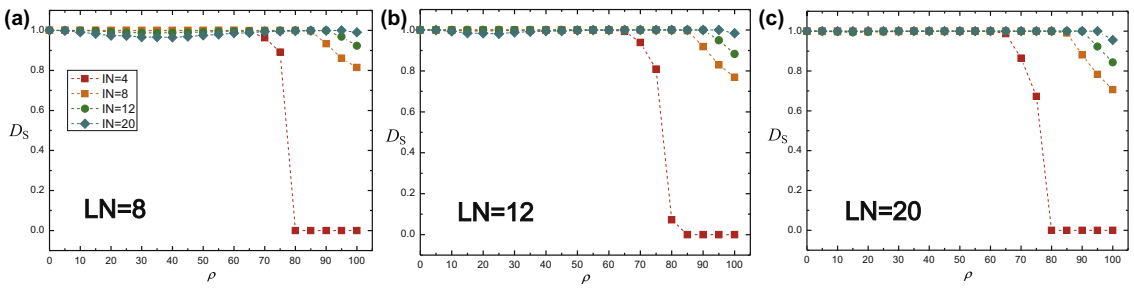

Fig. 8. The degree of stability D_s as a function of population density ρ. Each curve stands for a different interaction size. The learning size in (a)–(c) is 8, 12, 20, respectively; Network size $L = 200$.

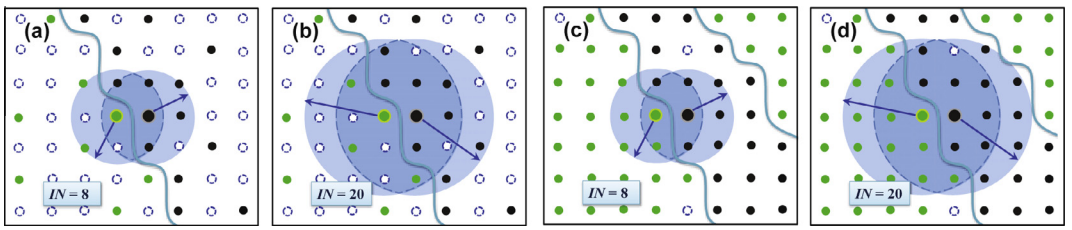

Fig. 9. The effect of interaction neighborhood size on a micro-level illustration, at a certain middle state. The blue line indicates the boundary of cooperators and defectors. For (a) and (b), population density $\rho = 40\%$, interaction size is 8 and 20, respectively; For (c) and (d), population density $\rho = 95\%$, interaction size is 8 and 20, respectively; Learning size is fixed at 8 and network size $L = 600$ in all cases. (For interpretation of the references to colour in this figure caption, the reader is referred to the web version of this article.)

of learning neighborhood, all the $LN = 4$ curves suffer a longer decrease period before the commencement of the rising stage.

Fig. 6 gives the variation of D_s over population density in other IN sizes. The role of learning neighborhood at each stage also applies in other interaction sizes. Larger learning size 'calms down' the turbulence of cooperator proportion at the beginning; as the community is gradually filled with more players, on the contrary, larger learning size destroys the tranquility and makes cooperators extinct more quickly. What is more, the network becomes unstable even at a smaller ρ as the interaction size increases.

3.2. Effect of interaction neighborhood

Fig. 7 presents how the cooperator fraction varies under different sizes of interaction neighborhood.

The 'wired' curves in (a) are the ones we discuss at the end of Section 3.1. Due to a limited range of learning neighbors, the strategy information is not well spread in the community, hence (a) is not considered in the following. In Fig. 7 (b)–(d), we see that the defectors corrupt cooperators via the enlargement of IN at the rising stage. However, interaction neighbors help maintain cooperation at the gliding stage.

To explore the role of interaction neighborhood on cooperation, we still use the conception of cooperator-cluster stability. Fig. 8 reveals the variation tendency of D_s in different interaction sizes. Take $LN = 8$ for instance, when some nodes are filled up with players ($\rho < 55\%$), larger interaction range disrupts the cooperator clusters and pulls down the fraction of cooperators (see Fig. 7(b), rising stage); however, as ρ continues to increase, interaction neighbors maintain the stability of the cooperator clusters and prohibits a further decrease in F_c (see Fig. 7(b), gliding stage). We can also find similar rules in Fig. 8(b) and (c). In addition, it is obvious to notice that a larger learning range as a 'sedative' is to alleviate the turbulence caused by the

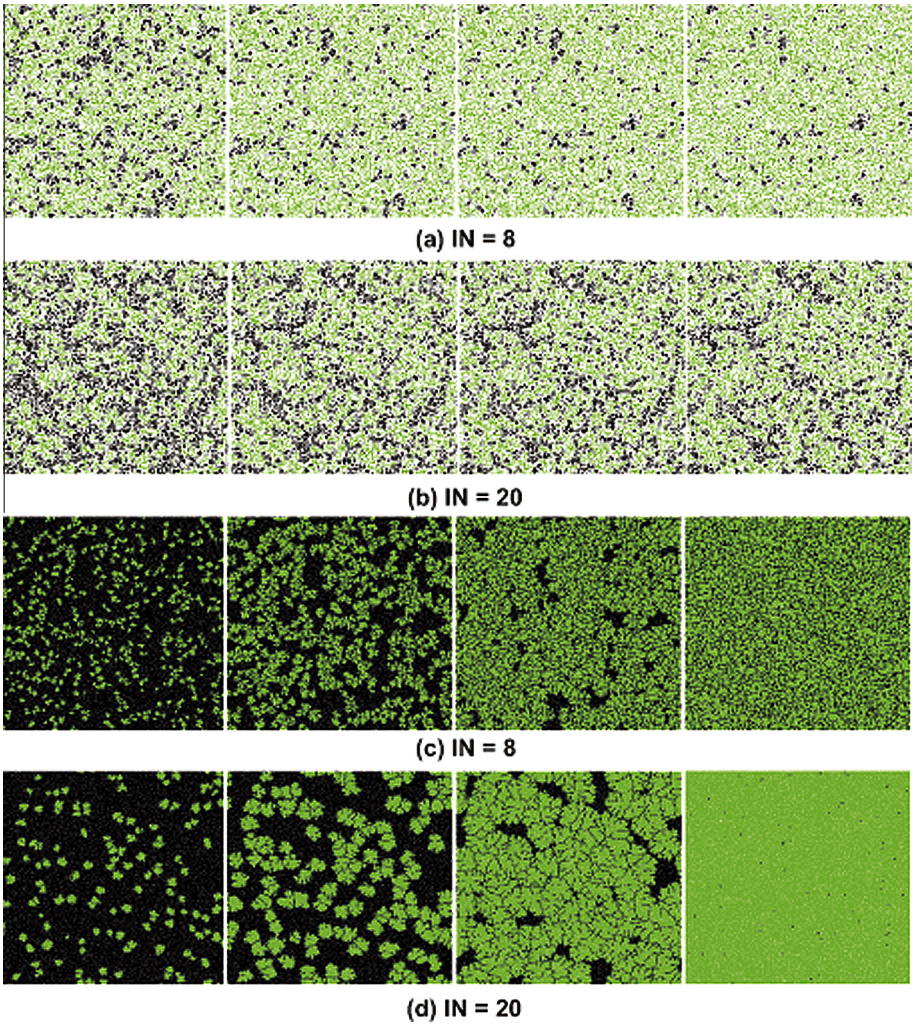

Fig. 10. The spatial patterns of cooperators (green), defectors (black) and empty sites (white) for four typical cases. Each row represents an intermediate state and the last figure in every row is the final state. Parameters are the same with those in Fig. 9, correspondingly. (For interpretation of the references to colour in this figure caption, the reader is referred to the web version of this article.)

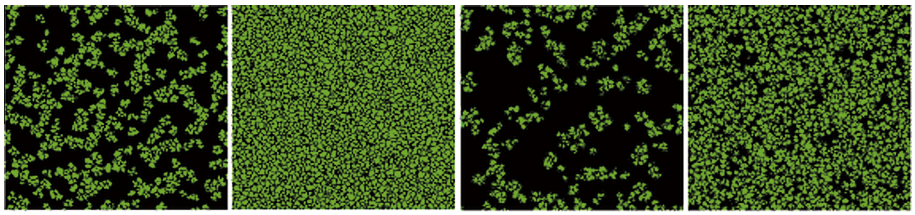

Fig. 11. Snapshot patterns of cooperators (green), defectors (black) and empty sites (white) when learning size is 8 and 20, respectively. The first and third is an intermediate state while the second and fourth is the final state. Interaction size is fixed to 20; population density $\rho = 100\%$; network size $L = 200$. (For interpretation of the references to colour in this figure caption, the reader is referred to the web version of this article.)

interaction neighbors at the rising stage; and that more learning neighbors corrupts the network at the gliding stage, both of which are already proven in Section 3.1.

To further investigate the effect of interaction neighborhood and vacant nodes, we dig into several cases on a micro level, as is shown in Fig. 9. The alteration of players' identities can only occur at the cooperator-defector boundary. When the learning size is constant, the motivation to lure cooperators to turn into defectors is the big payoff difference among them. In the overlapped area, every round the defector wins one more dollar than the cooperator does.

Consider two targets in the observing community, we calculate the payoff difference ($\Delta = P_C - P_D$) in Fig. 9 (a)–(d), centered on the cooperator at a certain intermediate state as follows:

$$\Delta_a = 2.45, \quad \Delta_b = -1.98, \quad \Delta_c = -1.33, \quad \Delta_d = 5.12 \qquad (7)$$

From Eq. (3) we know once the difference Δ tends to -2 or $+2$, cooperators will imitate defectors with probability of 100% or 0. When ρ is small, larger interaction range gets a bigger overlapped area, i.e, the cooperator takes parts in more rounds with the defector. Hence the payoff of defectors transcends that of cooperators ($\Delta_b < 0$); However, when ρ increases to 100%, for the cooperator, the non-overlapped part compensates for the payoff disadvantage whereas the defector gets little in its non-overlapped area. (Note that the compensation effect of the non-overlapped area is trivial when ρ is small.) Hence more interactive neighbors at the gliding stage guarantees enough cooperators to stick to their identities ($\Delta_d > 0$). We can predict that, in Fig. 9(d), cooperator clusters will squeeze the defectors and make their existence as a form of thin lines in the final state, which is proved later in Section 3.3.

3.3. Reviewing the problem via snapshot

After a comprehensive investigation of the influence of both interaction and learning neighbourhood on cooperative evolution, we try to unveil the mechanisms through snapshot patterns.

Fig. 10 shows how the interactive neighbors affect the formation of cooperator clusters. From the pattern we see that smaller interaction range at a smaller population density helps the propagation of altruism and forms stronger clusters to resist the exploitation of defectors (see Fig. 9(a) and (b)); while as ρ tends larger, larger interaction range helps the enlargement of cooperation clusters (see Fig. 9(c) and (d)). The process of the final cooperator-dominant state is clearly seen through dynamic simulations: first cooperators form a strong alliance through neighbor links; then they start to expand their realms and squeeze the defectors between clusters; finally the black spots can only exist in a form of thin lines or vanish if the conditions are proper. Although there might be occasionally identity alterations at the boundaries in the final state, the community is under a dynamical balance in the end.

Micro-level elaborations on the role of learning neighborhood is presented in Fig. 11. When the community is full of players, larger learning size destroys the cooperator-cluster stability. We can observe that, in $LN = 20$ case, there exist many 'burs' around the boundaries both at the intermediate and final state; whereas the boundaries in $LN = 8$ case are more neat and clear, demonstrating a robust stability of cooperator clusters. Actually, too much information flow caused by larger learning links gives free riders a good chance to lure cooperators to greater benefits.

4. Conclusion

In summary, we examine the influence of neighborhood size and type in the context of evolutionary spatial public goods game. The cooperator fraction as a function of population density shows a three-stage tendency. Through the conception of information flow rate, we investigate the role of learning neighborhood at the rising stage and find larger LN helps enhance the strategy transmission; The degree of stability measures how robust the cooperator cluster is and we find the role of learning neighborhood at the gliding stage is to make chaos among cooperators. Then we apply the stability theory in the study of the effect of interaction neighborhood. Quite opposite to learning neighborhood, we explore that larger IN destroys the cooperator cluster at the rising stage while more interactive neighbors alleviate the stability at the gliding stage. The conclusion can also be drawn via calculating the payoff difference at an intermediate state. At last, we verify what we have put forward via a micro-level explanation — snapshots. We find cooperator clusters squeeze the defectors into a form of line if the final state is cooperator-dominant; or two kind of players both form a stable cluster, i.e, a dynamical equilibrium. In addition, at the gliding stage, larger learning neighborhood causes more 'blurry burs' around the boundaries and thus makes more cooperators disappear easily. Current results are conducive to further

analyzing and understanding the emergence of cooperation in many natural, economic and social systems.

Acknowledgements

The authors acknowledge the funding support from the National Natural Science Foundation of China (Grant No. 61272173, No. 61100194, No. 71203017), the Fundamental Research Funds for Central Universities (Grant No. DUT12JR08, No. DUT13LK38).

References

[1] Gintis H. Game Theory Evolving. Princeton, NJ: Princeton University Press; 2000.
[2] Nowak MA. Evolutionary Dynamics: Exploring the Equations of Life. Cambrige, MA: Harvard Universtiy Press; 2006.
[3] Sigmund K. The Calculus of Selfishness. Princeton, NJ: Princeton University Press; 2010.
[4] Axelrod R. The Evolution of Cooperation. New York: Basic Books; 2006.
[5] Nowak MA. Five rules for the evolution of cooperation. Science 2006;314:1560–3.
[6] Szabó G, Szolnoki A, Perc M, Stark H. Impact of aging on the evolution of cooperation in the spatial prisoner's dilemma game. Phys Rev E 2009;80:021901.
[7] Wang Z, Wang Z, Zhu XD, Arenzon JJ. Cooperation and age structure in spatial games. Phys Rev E 2012;85:011149.
[8] Wang Z, Wang Z, Yang YH, Yu MX, Liao LG. Age-related preferential selection can promote cooperation in the prisoner's dilemma game. Int J Mod Phys C 2012;23:1250013.
[9] Szabó G, Tőke C. Evolutionary prisoner's dilemma game on a square lattice. Phys Rev E 1998;58:69–73.
[10] Santos FC, Pacheco JM. Scale-free networks provide a unifying framework for the emergence of cooperation. Phys Rev Lett 2005;95:098104.
[11] Wang Z, Szolnoki A, Perc M. Wisdom of groups promotes cooperation in evolutionary social dilemmas. Sci Rep 2012;2:576.
[12] Xia CY, Sanro M, Moreno Y. Effects of environment knowledge on agglomeration and cooperation in spatial public goods games. Adv Complex Syst 2012;15:1250056.
[13] Jin Q, Wang Z, Wang Z, Wang YL. Strategy changing penalty promotes cooperation in spatial prisoner's dilemma game. Chaos Solitons Fract 2012;45:395–401.
[14] Szabó G, Vukov J, Szolnoki A. Phase diagrams for an evolutionary prisoner's dilemma game on two-dimensional lattices. Phys Rev E 2005;72:047107.
[15] Vukov J, Szabó G, Szolnoki A. Cooperation in the noisy case: prisoner's dilemma game on two types of regular random graphs. Phys Rev E 2006;73:067103.
[16] Perc M. Double resonance in cooperation induced by noise and network variation for an evolutionary prisoner's dilemma. New J Phys 2006;8:183.
[17] Zhang GQ, Sun QB, Wang L. Noise-induced enhancement of network reciprocity in social dilemmas. Chaos Solitons Fract 2013;51:31–5.
[18] Szolnoki A, Szabó G. Cooperation enhanced by inhomogeneous activity of teaching for evolutionary prisoner's dilemma games. EPL 2007;77:30004.
[19] Wang Z, Wang L, Yin ZY, Xia CY. Inferring reputation promotes the evolution of cooperation in spatial social dilemma games. PLoS one 2012;7:e40218.
[20] Perc M, Szolnoki A, Szabó G. Restricted connections among distinguished players support cooperation. Phys Rev E 2008;78:066101.
[21] Du WB, Cao XB, Hu MB, Wang WX. Asymmetric cost in snowdrift game on scale-free networks. EPL 2009;87:60004.
[22] Xia CY, Ma ZQ, Wang YL, Wang JS, Chen ZQ. Enhancement of cooperation in prisoner's dilemma game on weighted lattices. Physica A 2011;390:4602–9.
[23] Xia CY, Zhao J, Wang J, Wang YL, Zhang H. Influence of vertex weight on cooperative behavior in a spatial snowdrift game. Phys. Scr. 2011;85:025802.
[24] Ma ZQ, Xia CY, Sun SW, Wang L, Wang HB, Wang J. Heterogeneous link weight promotes the cooperation in spatial prisoner's diemma. Int J Mod Phys C 2011;22:1257–68.
[25] Zhang JJ, Ning HY, Yin ZY, Sun SW, Wang L, Sun JQ, et al. A novel snowdrift game model with edge weighting mechanism on the square lattice. Front Phys 2012;7:366–73.
[26] Wang Z, Murks A, Du WB, Rong ZH, Perc M. Coveting thy neighbors fitness as a means to resolve social dilemmas. J Theor Biol 2011;277:19–26.
[27] Xia CY, Ma ZQ, Wang Z, Wang J. Evaluating fitness by integrating the highest payoff within the neighborhood promotes the cooperation in social dilemmas. Physica A 2012;391:6440–7.
[28] Wang Z, Perc M. Aspiring to the fittest and promotion of cooperation in the prisoner's dilemma game. Phys Rev E 2010;82:021115.
[29] Roca CP, Cuesta JA, Sanchez A. Time scales in evolutionary dynamics. Phys Rev Lett 2006;97:158701.
[30] Nowak MA, May RM. Evolutionary games and spatial chaos. Nature 1992;359:826–9.
[31] Szolnoki A, Perc M, Szabó G. Topology-independent impact of noise on cooperation in spatial public goods games. Phys Rev E 2009;80:056109.
[32] Nowak MA, Bonhoeffer S, May RM. Spatial games and the maintenance of cooperation. PNAS 1994;91:4877–81.
[33] Szolnoki A, Perc M. Group-size effects on the evolution of cooperation in the spatial public goods game. Phys Rev E 2011;84:047102.
[34] Santos FC, Rodrigues JF, Pacheco JM. Graph topology plays a determinant role in the evolution of cooperation. PNAS 2006;273:51–5.
[35] Szabó G, Fáth G. Evolutionary games on graphs. Phys Rep 2007;446:97–216.
[36] Wang L, Xia CY, Wang J. Coevolution of network structure and cooperation in the public goods game. Phys Scr 2013;87:055001.
[37] Perc M, Gómez-Gardeñes J, Szolnoki A, Floría LM, Moreno Y. Evolutionary dynamics of group interactions on structured populations: a review. J R Soc Interface 2013;10:20120997.
[38] Zhang JJ, Wang J, Wang L, Sun SW, Wang Z, Xia CY. Effect of growing size of interaction neighbors on the evolution of cooperation in spatial snowdrift game. Commun Theor Phys 2012;57:541C546.
[39] Ifti M, Killingback T, Doebeli M. Effects of neighbourhood size and connectivity on spatial continuous prisoner's dilemma. J Theor Biol 2004;231:97–106.
[40] Vainstein MH, Arenzon JJ. Disordered environments in spatial games. Phys Rev E 2001;64:051905.
[41] Wang Z, Szolnoki A, Perc M. Percolation threshold determines the optimal population density for public cooperation. Phys Rev E 2012;85:037101.
[42] Wang Z, Szolnoki A, Perc M. If players are sparse social dilemmas are too: importance of percolation for evolution of cooperation. Sci Rep 2012;2:369.
[43] Xia CY, Miao Q, Zhang JJ. Impact of neighborhood separation on the spatial reciprocity in the prisoner's dilemma game. Chaos Solitons Fract 2013;51:22–30.
[44] Wu ZX, Wang YH. Cooperation enhanced by the difference between interaction and learning neighborhoods for evolutionary spatial prisoner's dilemma games. Phys Rev E 2007;75:041114.
[45] Xu ZJ, Wang Z, Zhang LZ. Self-adjusting rule in spatial voluntary public goods games. EPL 2010;90:20001.
[46] Hauert C, Doebeli M. Spatial structure often inhibits the evolution of cooperation in the snowdrift game. Nature 2004;428:643–6.
[47] Xiao RB, Zhang YF. Cooperative evolution of spatial games with unsymmetrical neighborhoods in disordered environment. Adv Sci Lett 2012;16:27–31.